Available online at www.sciencedirect.com
SCIENCE DIRECT®
Journal of Solid State Chemistry 171 (2003) 137–142
JOURNAL OF SOLID STATE CHEMISTRY
http://elsevier.com/locate/jssc

Lanthanum gallium manganese antimonide $La_{12}Ga_{3.5}Mn_{0.5}Sb_{23.5}$

Shane J. Crerar, Mark G. Morgan, and Arthur Mar*

Department of Chemistry, University of Alberta, Edmonton, Alta., Canada T6G 2G2

Received 14 April 2002; received in revised form 10 July 2002; accepted 17 November 2002

Abstract

Lanthanum gallium manganese antimonide $La_{12}Ga_{3.5}Mn_{0.5}Sb_{23.5}$ is the first quaternary rare-earth antimonide containing a p-block metal and a transition metal. It has been synthesized by reaction of the elements and its structure has been determined by single-crystal X-ray diffraction methods (orthorhombic, space group $D_{2h}^{25} - Immm$, $Z = 2$, $a = 4.3534(11)$ Å, $b = 19.814(5)$ Å, $c = 26.977(7)$ Å). $La_{12}Ga_{3.5}Mn_{0.5}Sb_{23.5}$ is a stuffed variant of the $RE_{12}Ga_4Sb_{23}$-type structure: isolated $GaSb_3$ trigonal planes are located within groupings of La_6 trigonal prisms that are surrounded by five- and six-atom wide Sb ribbons, which are connected by Ga_2 pairs, $GaSb_6$ octahedra, or $MnSb_4$ tetrahedra. The electrical resistivity along a is $3.0 \times 10^{-3}\,\Omega$ cm at room temperature and shows little temperature dependence.

Keywords: Antimonide; Lanthanum; Gallium; Manganese; Crystal structure

1. Introduction

Ternary rare-earth antimonides $RE_xM_ySb_z$ present interesting possibilities for bonding when M is a p-block metal of similar electronegativity to Sb [1]. Their structures show features characteristic of intermetallic compounds, such as high coordination numbers and disorder, but may also contain recognizable molecular entities such as Ga_6 rings in $La_{13}Ga_8Sb_{21}$, Ga_2 pairs in $RE_{12}Ga_4Sb_{23}$, or $GaSb_3$ trigonal planes in both [2]. A wide variety of anionic Sb substructures are also present in these compounds. In the complicated $RE_{12}Ga_4Sb_{23}$ structure, there exists an essentially empty site that corresponds to the location of a Mn atom in the RE_6MnSb_{15} structure [3], which is related to $RE_{12}Ga_4Sb_{23}$ through what appears to be a homologous series. We thus considered the possibility that $RE_{12}Ga_4Sb_{23}$ could serve as a host for an interstitial structure in which guest atoms such as Mn could be stuffed into these vacant sites. Such a target compound would have a composition $RE_{12}Ga_4Mn_4Sb_{23}$ if all the sites were fully occupied. However, since the $RE_{12}Ga_4Sb_{23}$ structure contains Ga_2 pairs whereas the RE_6MnSb_{15} structure contains Sb_2 pairs, it is not obvious whether introduction of interstitial Mn atoms would also entail disorder of these atom pairs.

To test our predictions, we investigated the mixed $La_{12}Ga_xMn_ySb_{23}$ system to see if a quaternary compound could be prepared. We describe here the synthesis and structure of $La_{12}Ga_{3.5}Mn_{0.5}Sb_{23.5}$. Although Mn can indeed be stuffed into $La_{12}Ga_4Sb_{23}$, doing so causes unforeseen distortions in the rest of the host structure. Quaternary rare-earth antimonides containing two different p-block metals have recently been reported [1,4]; to our knowledge, $La_{12}Ga_{3.5}Mn_{0.5}Sb_{23.5}$ is the first quaternary rare-earth antimonide containing a p-block and a transition metal.

2. Experimental

2.1. Synthesis

A 0.25-g mixture of La powder (99.9%, Cerac), crushed Ga granules (99.99%, Alfa-Aesar), Mn powder (99.95%, Cerac), and Sb powder (99.995%, Aldrich) in the ratio 12:4:2:23 was loaded into an evacuated fused-silica tube (5-cm length; 10-mm i.d.). The sample was heated at 1000°C for 3 days, cooled to 600°C over 1 day, heated at 600°C for 3 days, and then cooled to 20°C over 12 h. Grey needle-shaped crystals were obtained with an

*Corresponding author. Fax: +1-780-492-8231.
E-mail address: arthur.mar@ualberta.ca (A. Mar).

0022-4596/03/$ - see front matter © 2003 Elsevier Science (USA). All rights reserved.
doi:10.1016/S0022-4596(02)00200-1

elemental composition (mol%) of 28(1) La, 8(1) Ga, 2(1) Mn, and 62(1) Ga (average of 2 analyses), determined by energy-dispersive X-ray (EDX) analysis on a JEOL JSM-6301FXV scanning electron microscope.

2.2. Structure determination

X-ray diffraction data were collected on a Bruker Platform/SMART 1000 CCD diffractometer at 22°C with a combination of ϕ rotations (0.3°) and ω scans (0.3°) in the range $2° \leqslant 2\theta(\mathrm{Mo}K\alpha) \leqslant 65°$. Final cell parameters were refined from least-squares analysis of 912 reflections. Crystal data and further details of the data collection are given in Table 1. All calculations were carried out using the SHELXTL (Version 5.1) package [5]. Conventional atomic scattering factors and anomalous dispersion corrections were used [6]. Intensity data were processed, and face-indexed numerical absorption corrections were applied in XPREP.

The Laue symmetry *mmm* and the systematic extinctions ($hkl: h+k+l=2n+1$) suggested orthorhombic space groups *Immm*, *Imm*2, *I*222, and $I2_12_12_1$. On the basis of the similarity of their intensity patterns, the centrosymmetric space group *Immm* was chosen and initial positions for the La and Sb atoms in $La_{12}Ga_{3.5}Mn_{0.5}Sb_{23.5}$ were taken from the $Pr_{12}Ga_4Sb_{23}$ structure (2). The remaining atoms were located in difference electron density maps. The Ga(1) site, coordinated in a trigonal planar fashion by Sb atoms, was initially refined at 0, 0, ~0.19 but displayed a thermal ellipsoid highly elongated along the *a*-direction. This site was thus shifted off the mirror plane into two half-occupied split sites, resulting in more reasonable atomic displacement parameters. Attempts to refine the structure in *I*2*mm* did not support an ordered structure in which the pyramidal distortion of the $GaSb_3$ trigonal planes occurs exclusively in one direction. As predicted, additional electron density was revealed at the tetrahedral site at 0, ~0.18, $\frac{1}{2}$, which was assigned as Mn. Occupation of Ga(3) site at 0, ~0.43, 0 gives rise to Ga_2 pairs. However, two additional sites were inferred by the presence of electron density along 0, *y*, 0 that are too close to the Ga(3) site for all of them to be fully occupied simultaneously. Taking into account the EDX analyses indicating a much higher proportion of Ga to Mn and armed with a knowledge of reasonable bond lengths and geometries from literature precedent, we considered various models involving disorder of Ga, Mn, and Sb atoms. Refinement of occupancies resulted in values of 47(3)% for Ga(3) on one hand, and 29(2)% for Ga(2), 32(2)% for Sb(9), and 19(2)% for Mn on the other hand, although caution has to be exercised in accepting these values because of their high correlation with the displacement parameters. The most chemically sensible interpretation suggests that there are Ga_2 pairs on one hand (50%), and a combined unit connecting a $GaSb_6$ octahedron with a $MnSb_4$ tetrahedron, oriented in opposite directions along *b*, on the other hand (each 25%). The formula for this model is "$La_{12}Ga_{3.5}Mn_{0.5}Sb_{23.5}$," corresponding to a composition (30% La, 9% Ga, 1% Mn, 59% Sb) in good agreement with the elemental analysis given earlier.

Table 1
Crystallographic data for $La_{12}Ga_{3.5}Mn_{0.5}Sb_{23.5}$

Formula	$La_{12}Ga_{3.5}Mn_{0.5}Sb_{23.5}$
Formula mass (amu)	4799.54
Space group	$D_{2h}^{25}-Immm$ (No. 71)
a (Å)[a]	4.3534(11)
b (Å)[a]	19.814(5)
c (Å)[a]	26.977(7)
V (Å^3)	2327.0(10)
Z	2
ρ_{calcd} (g cm^{-3})	6.850
Crystal dimensions (mm)	$0.234 \times 0.010 \times 0.010$
Radiation	Graphite monochromated Mo$K\alpha$, $\lambda = 0.71073$ Å
μ(Mo$K\alpha$) (cm^{-1})	262.12
Transmission factors	0.368–0.785
2θ limits	$2.56° \leqslant 2\theta$ (Mo$K\alpha$) $\leqslant 64.52°$
Data collected	$-6 \leqslant h \leqslant 6$, $-29 \leqslant k \leqslant 24$, $-39 \leqslant l \leqslant 40$
No. of data collected	12243
No. of unique data, including $F_o^2 < 0$	2369
No. of unique data, with $F_o^2 > 2\sigma(F_o^2)$	1100
No. of variables	76
$R(F)$ for $F_o^2 > 2\sigma(F_o^2)$[b]	0.071
$R_w(F_o^2)$[c]	0.173
Goodness of fit	0.934
$(\Delta\rho)_{max}$, $(\Delta\rho)_{min}$ (e Å^{-3})	6.98, –2.92

[a] Obtained from a refinement constrained so that $\alpha = \beta = \gamma = 90°$.
[b] $R(F) = \sum||F_o| - |F_c||/\sum|F_o|$.
[c] $R_w(F_o^2) = [\sum[w(F_o^2-F_c^2)^2]/\sum wF_o^4]^{1/2}$; $w^{-1} = [\sigma^2(F_o^2)+(0.0702p)^2]$ where $p = [\max(F_o^2, 0) + 2F_c^2]/3$.

Ga(2), Ga(3), and Sb(9) were refined with isotropic displacement parameters only. For all other atoms, the final refinement led to reasonable anisotropic displacement parameters. The largest residuals in the difference electron density map ($\Delta\rho_{max} = 6.98$; $\Delta\rho_{min} = -2.92$ e Å^{-3}) are located less than 0.5 Å away from the Ga(2) site. Final values of the positional and displacement parameters are given in Table 2. Interatomic distances are listed in Table 3. Further data, in the form of a CIF, have been sent to Fachinformationszentrum Karlsruhe, Abt. PROKA, 76344 Eggenstein-Leopoldshafen, Germany, as supplementary material No. CSD–412762 and can be obtained by contacting FIZ (quoting the article details and the corresponding CSD numbers).

2.3. Electrical resistivity

Several crystals confirmed to be $La_{12}Ga_{3.5}Mn_{0.5}Sb_{23.5}$ by EDX analyses were mounted in a four-probe

Table 2
Positional and equivalent isotropic displacement parameters for $La_{12}Ga_{3.5}Mn_{0.5}Sb_{23.5}$

Atom	Wyckoff position	Occupancy	x	y	z	U_{eq} or U_{iso} (Å^2)[a]
La(1)	8*l*	1	0	0.27770(7)	0.40555(6)	0.0119(3)
La(2)	8*l*	1	0	0.38876(8)	0.26283(5)	0.0110(3)
La(3)	4*j*	1	$\frac{1}{2}$	0	0.09345(8)	0.0110(4)
La(4)	4*j*	1	$\frac{1}{2}$	0	0.37901(8)	0.0154(5)
Ga(1)	8*m*	0.50	0.045(5)	0	0.18918(19)	0.018(4)
Ga(2)	4*g*	0.25	0	0.3791(10)	0	0.025(4)
Ga(3)	4*g*	0.50	0	0.4318(5)	0	0.0195(19)
Mn	4*h*	0.25	0	0.1789(14)	$\frac{1}{2}$	0.027(6)
Sb(1)	8*l*	1	0	0.10970(10)	0.42924(9)	0.0255(5)
Sb(2)	8*l*	1	0	0.11450(10)	0.14083(6)	0.0126(4)
Sb(3)	8*l*	1	0	0.22264(9)	0.28595(7)	0.0136(4)
Sb(4)	8*l*	1	0	0.33342(9)	0.14459(6)	0.0140(4)
Sb(5)	4*i*	1	0	0	0.28741(9)	0.0136(5)
Sb(6)	4*h*	1	0	0.38526(14)	$\frac{1}{2}$	0.0209(6)
Sb(7)	4*g*	1	0	0.23047(14)	0	0.0169(6)
Sb(8)	2*a*	1	0	0	0	0.0124(7)
Sb(9)	4*g*	0.25	0	0.4686(7)	0	0.027(3)

[a] U_{eq} is defined as one-third of the trace of the orthogonalized U_{ij} tensor. The closely spaced, partially occupied sites Ga(2), Ga(3), and Sb(9) were refined with isotropic displacement parameters only.

Table 3
Selected interatomic distances (Å) in $La_{12}Ga_{3.5}Mn_{0.5}Sb_{23.5}$

La(1)–Mn	3.214(17)	La(4)–Ga(3)	3.533(5) (× 2)
La(1)–Sb(2)	3.296(2) (× 2)	La(4)–Sb(5)	3.293(2) (× 2)
La(1)–Sb(6)	3.322(2)	La(4)–Sb(9)	3.323(3) (× 2)
La(1)–Sb(7)	3.355(1) (× 2)	La(4)–Sb(1)	3.361(2) (× 4)
La(1)–Sb(4)	3.379(2) (× 2)	La(4)–Sb(4)	3.362(2) (× 2)
La(1)–Sb(1)	3.389(3)	Ga(1)–Sb(2)	2.624(4) (× 2)
La(1)–Sb(3)	3.406(2)	Ga(1)–Sb(5)	2.657(6)
La(2)–Ga(1)	3.234(15) (× 2)	Ga(2)–Sb(1)	2.904(2) (× 4)
La(2)–Ga(1)	3.487(16) (× 2)	Ga(2)–Sb(7)	2.95(2)
La(2)–Sb(3)	3.350(2)	Ga(2)–Sb(9)	3.02(2)
La(2)–Sb(3)	3.368(2) (× 2)	Ga(3)–Ga(3)	2.70(2)
La(2)–Sb(4)	3.373(2)	Ga(3)–Sb(1)	3.010(3) (× 4)
La(2)–Sb(5)	3.381(2) (× 2)	Mn–Sb(1)	2.350(16) (× 2)
La(2)–Sb(2)	3.391(2) (× 2)	Mn–Sb(7)	2.822(18) (× 2)
La(3)–Ga(1)	3.255(15) (× 2)	Sb(1)–Sb(4)	3.158(2) (× 2)
La(3)–Ga(1)	3.506(16) (× 2)	Sb(1)–Sb(9)	3.285(7) (× 2)
La(3)–Sb(8)	3.331(2) (× 2)	Sb(3)–Sb(4)	3.079(2) (× 2)
La(3)–Sb(2)	3.394(2) (× 4)	Sb(3)–Sb(3)	3.111(3) (× 2)
La(3)–Sb(6)	3.395(3) (× 2)	Sb(6)–Sb(8)	3.148(2) (× 2)
		Sb(6)–Sb(7)	3.162(3) (× 2)

configuration for AC resistivity measurements along the needle axis *a* between 2 and 300 K on a Quantum Design PPMS system equipped with an AC-transport controller (Model 7100). The crystals averaged 0.6 mm in length and 0.001 mm^2 in cross-sectional area. A current of 0.1 mA and a frequency of 16 Hz were used.

3. Results and discussion

The structure of $La_{12}Ga_{3.5}Mn_{0.5}Sb_{23.5}$, the first quaternary antimonide containing both a p-block metal and a transition metal, is shown viewed down the short *a*-axis in Fig. 1. In common with the growing number of ternary rare-earth main-group antimonides, it contains a variety of anionic substructures involving homoatomic bonding of the main-group components (1). The Sb atoms are arranged in five-atom-wide (Sb(7)–Sb(6)–Sb(8)–Sb(6)–Sb(7)) and six-atom-wide (Sb(1)–Sb(4)–Sb(3)–Sb(3)–Sb(4)–Sb(1)) ribbons that extend down the *a*-axis. These ribbons outline large channels containing trigonal prisms of the La atoms, which are connected to form a larger four-prism assembly and share their trigonal faces to form columns running along the *a*-axis. Centred within these trigonal prisms are additional Ga and Sb atoms, which are bonded to give slightly pyramidally distorted $GaSb_3$ units. The most complicated part of the structure involves the linking of the Sb ribbons. The terminal atoms at the borders of these ribbons are Sb(1) and Sb(7). As shown in Fig. 2, there are three scenarios. Occupation of the Ga(3) sites results in Ga_2-pairs that link together the six-atom-wide Sb ribbons, leaving the five-atom-wide ribbons isolated (Fig. 2(a)). The coordination of a Ga(3) atom is thus square pyramidal, with Sb(1) atoms at the base and another Ga(3) atom at the apex. Alternatively, the Ga(2) and Sb(9) sites could be occupied, giving rise to an octahedral coordination around Ga. Simultaneously, there are tetrahedral sites occupied by Mn atoms. Disorder is entailed by the two possible orientations of the combined octahedral $GaSb_6$/tetrahedral $MnSb_4$ unit (Fig. 2(b) and (c)), as well as between these units and the Ga_2-pairs (Fig. 2(a)).

The Sb–Sb distances within the Sb ribbons range from 3.079(2) to 3.162(3) Å, consistent with similar distances found in ribbons and square sheets in other antimonides (1). If bond valences are calculated from the formula

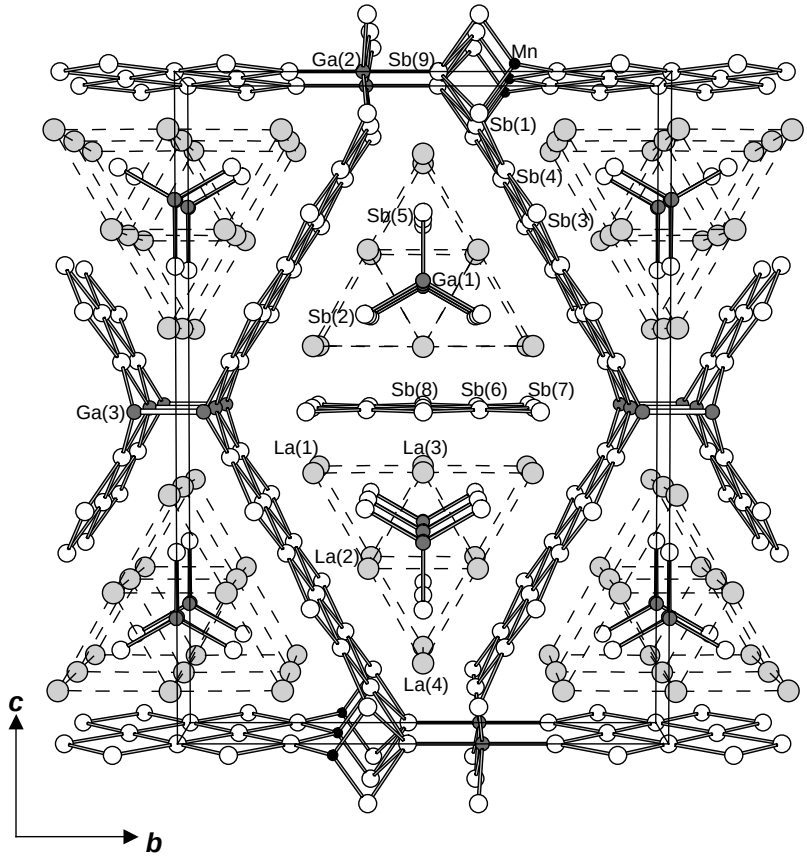

Fig. 1. View of $La_{12}Ga_{3.5}Mn_{0.5}Sb_{23.5}$ down the *a*-axis showing the unit cell outline and the labelling scheme. The large lightly shaded circles are La atoms, the medium solid circles are Ga atoms, the small solid circles are Mn atoms, and the medium open circles are Sb atoms. The dashed lines outline the assemblies of La_6 trigonal prisms. One possible local ordering of the Ga_2 pairs and the octahedral $GaSb_6$/tetrahedral $MnSb_4$ units is portrayed.

$v_{ij} = \exp[(2.80-d_{ij})/0.37]$, where 2.80 Å is chosen as the bond valence parameter for an Sb–Sb single bond [7,8], then the distances above correspond to valences ranging from 0.47 to 0.38. These values bear out the usual interpretation that these are approximately one-electron bonds, and are supported by more rigorous calculation of overlap populations from band structure determinations [9,10]. The 3.285(7) Å distance between Sb(9) and Sb(1) is long, but its bond valence of 0.27 still implies considerable strength. After all, it is still shorter than the interlayer Sb–Sb distance found in elemental Sb of 3.355 Å [11], which has been demonstrated to be significant.

It is interesting that the $GaSb_3$ units are distorted from planarity, the Ga(1) atoms lying 0.20(2) Å above or below the plane of the three Sb atoms. In $La_{13}Ga_8Sb_{21}$, a distortion of similar magnitude is also observed [1]. In other compounds, the $GaSb_3$ units are rigorously planar, as in Cs_6GaSb_3 [12], but even in the more closely related structure of $Pr_{12}Ga_4Sb_{23}$, the tendency to pyramidalize is manifested by an elongated thermal ellipsoid [2]. There is evidence that the Ga–Sb bonds in these units contain a significant π contribution involving back-donation from Sb orbitals into an empty *p* orbital on Ga [13]; indeed, the 2.624(4)–2.657(6) Å distances in $La_{12}Ga_{3.5}Mn_{0.5}Sb_{23.5}$ are shorter than those (2.709(2)–2.752(5) Å) in the $GaSb_4$ tetrahedra found in $Na_3Sr_3GaSb_4$ [14], for which only σ bonding can be operative. However, the distortion from planarity indicates a buildup of electron density on the Ga atom. The degree of distortion observed suggests that the Ga(1) atom in $La_{12}Ga_{3.5}Mn_{0.5}Sb_{23.5}$ is somewhat more reduced than it is in the related $Pr_{12}Ga_4Sb_{23}$ structure. The remaining Ga atoms reside in sites of higher CN and the Ga–Sb distances are even longer. The Ga(2) atom is surrounded octahedrally by Sb atoms at distances of 2.904(2)–3.02(2) Å. It resembles a Ge site in $La_6Ge_{5-x}Sb_{11+x}$ that is strongly displaced so that the four equatorial Ge–Sb distances are 2.9320(8) Å but the axial distances are 2.743(2) and 3.595(3) Å [15]. The Ga(3) atom is 3.010(3) Å away from four Sb atoms and 2.70(2) Å from another Ga(3) atom. These long Ga–Sb and Ga–Ga distances correspond to relatively weak bonds, which may be a matrix effect arising from the need to satisfy ionic interactions with the La atoms in the structure. The coordination geometries of the rare-earth atoms are bicapped square antiprisms, similar to that in $Pr_{12}Ga_4Sb_{23}$, with La–Sb distances of 3.293(2)

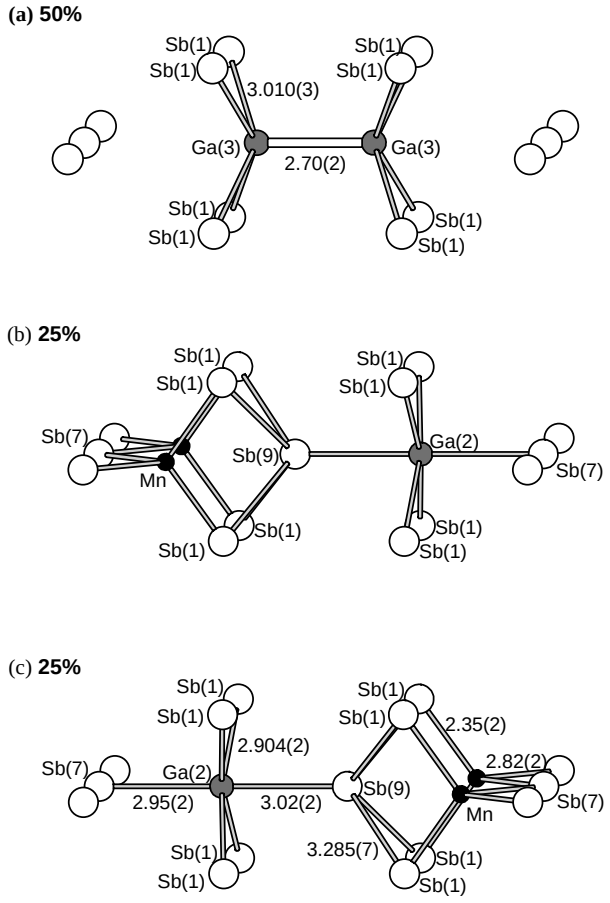

Fig. 2. Occupation of sites linking the five- and six-atom-wide Sb ribbons in $La_{12}Ga_{3.5}Mn_{0.5}Sb_{23.5}$.

–3.406(2) Å and La–Ga distances of 3.234(15)–3.533(5) Å, similar to those found in $LaSb_2$ (3.183–3.432 Å) [16] and $LaGa_2$ (3.335 Å) [17].

Fig. 3 shows the close relationship between the orthorhombic structures of La_6MnSb_{15} (3), $Pr_{12}Ga_4Sb_{23}$ (2), and $La_{12}Ga_{3.5}Mn_{0.5}Sb_{23.5}$. All contain assemblies of filled rare-earth trigonal prisms, a common motif in the structures of intermetallic compounds, surrounded by Sb ribbons. La_6MnSb_{15} contains single-prism columns whereas $Pr_{12}Ga_4Sb_{23}$ and $La_{12}Ga_{3.5}Mn_{0.5}Sb_{23.5}$ contain four-prism columns. The Sb ribbons in La_6MnSb_{15} are connected through Sb_2 pairs and $MnSb_4$ tetrahedra. In contrast, the Sb ribbons in $Pr_{12}Ga_4Sb_{23}$ are connected by Ga_2 pairs and the tetrahedral sites remain essentially vacant. In $La_{12}Ga_{3.5}Mn_{0.5}Sb_{23.5}$, the Sb ribbons are connected by a combination of Ga_2 pairs, $MnSb_4$ tetrahedra, and $GaSb_6$ octahedra. The appearance of the $GaSb_6$ octahedra is equivalent to linking the Sb ribbons by GaSb pairs. Disorder of the Ga and Sb atoms linking these ribbons is understandable given what is observed in the structures of La_6MnSb_{15} and $Pr_{12}Ga_4Sb_{23}$, and is analogous to the disorder of Ge and Sb atoms in $RE_6Ge_{5+x}Sb_{11+x}$ [15] and some quaternary stuffed iron germanium

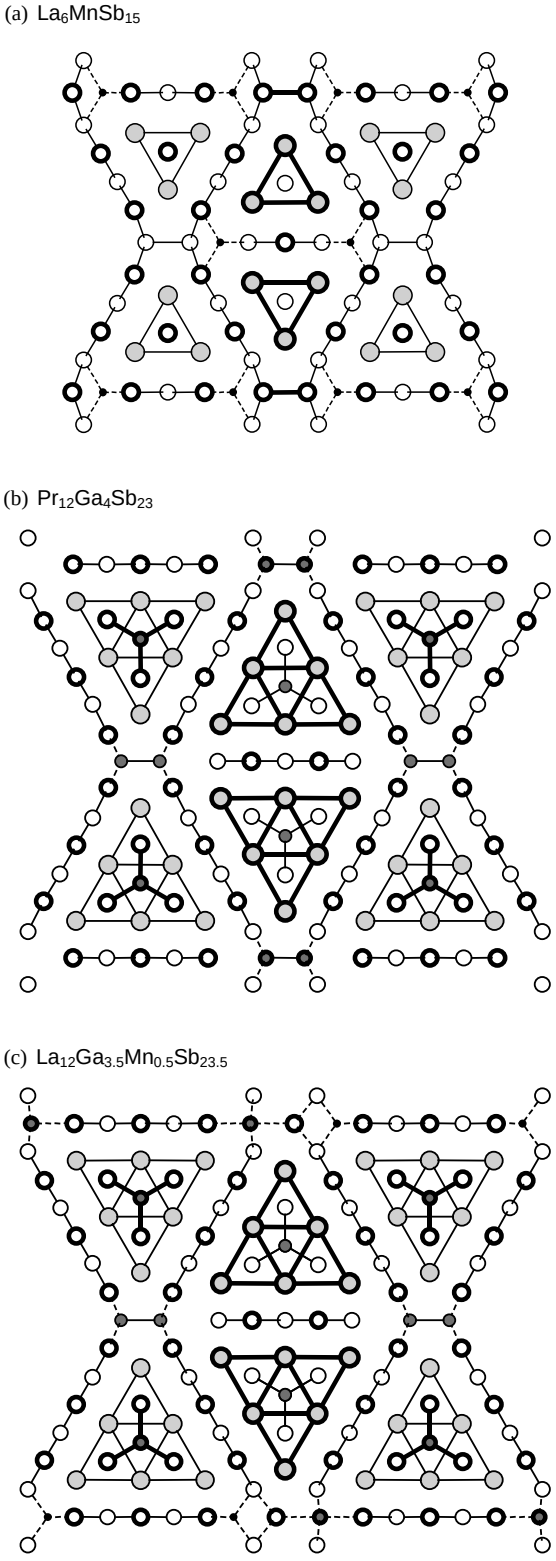

Fig. 3. Comparison of the structures of (a) La_6MnSb_{15}, (b) $Pr_{12}Ga_4Sb_{23}$, and (c) $La_{12}Ga_{3.5}Mn_{0.5}Sb_{23.5}$ shown in projection down the shortest axis. The large lightly shaded circles are rare-earth atoms, the medium solid circles are Ga atoms, the small solid circles are Mn atoms, and the medium open circles are Sb atoms. Circles with thicker rims are atoms residing in planes displaced by $\frac{1}{2}$ the short axis parameter.

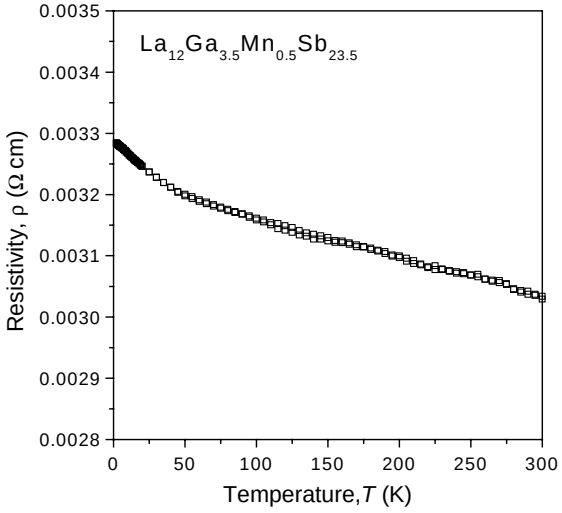

Fig. 4. Temperature dependence of the resistivity of $La_{12}Ga_{3.5}Mn_{0.5}Sb_{23.5}$.

antimonides [18]. In La_6MnSb_{15}, the Mn coordination can also be described as distorted bicapped tetrahedral if, in addition to two short (2.451(2) Å) and two long (2.843(1) Å) Mn–Sb bonds, the next two slightly longer (2.941(1) Å) distances are included. In $La_{12}Ga_{3.5}Mn_{0.5}Sb_{23.5}$, the distortion of the Mn coordination is even more severe so that the two longest Mn–Sb distances (3.64(2) Å) can be neglected, the remaining four Mn–Sb bonds (2.35(2), 2.82(2) Å) rendering the coordination geometry as a distorted tetrahedron. The recently described $(U_{0.5}Ho_{0.5})_3Sb_7$ also resembles these structures, but here the Sb ribbons are connected by single Sb atoms [19].

Although there are recognizable entities such as $[GaSb_3]^{6-}$ trigonal planes, isoelectronic with boron trihalides, and one-dimensional "non-classical" $[Sb_5]^{7-}$ ribbons, for which electron-counting rules have now been devised [9,10], the disorder between the Ga_2 pairs, GaSb pairs, and $MnSb_4$ tetrahedra makes it extremely difficult to formulate an overall charge distribution for such a complicated structure. Simple electron counting schemes are problematic to apply when the deviation from planarity of the $GaSb_3$ units suggests partial reduction of the Ga centre, and when Sb–Sb bonds within the Sb ribbons can vary over a wide range to accommodate non-integral numbers of electrons [13].

Fig. 4 shows a typical plot for the resistivity of $La_{12}Ga_{3.5}Mn_{0.5}Sb_{23.5}$, which increases only slightly with decreasing temperature ($\rho_{300} = 3.0 \times 10^{-3}\,\Omega\,cm$; $\rho_2 = 3.3 \times 10^{-3}\,\Omega\,cm$). Characteristic of disordered intermetallic compounds, the resistivity ratio is quite small, $\rho_{300}/\rho_2 = 0.91$. A band structure calculation performed for $La_{12}Ga_4Sb_{23}$ suggests that metallic behaviour should still be retained by small changes in electron count [13]. However, the severe disorder in $La_{12}Ga_{3.5}Mn_{0.5}Sb_{23.5}$ may well introduce many localized states that will destroy metallic conduction.

The planned preparation of $La_{12}Ga_{3.5}Mn_{0.5}Sb_{23.5}$ illustrates that $RE_{12}Ga_4Sb_{23}$ can indeed serve as a host structure to accommodate interstitial atoms. It is worthwhile attempting to fill the distorted tetrahedral sites by other transition metal atoms such as Cu and Zn, which can substitute for Mn in the La_6MnSb_{15} structure [3]. The similarity of $RE_6Ge_{5-x}Sb_{11+x}$ to these compounds also suggests the substitution of Ge for Ga to form other quaternary rare-earth transition metal main-group antimonides.

Acknowledgments

The Natural Sciences and Engineering Research Council of Canada and the University of Alberta supported this work. We thank Dr. Michael J. Ferguson (X-ray Crystallography Laboratory) for the data collection and George D. Braybrook for assistance with the EDX analysis.

References

[1] A.M. Mills, R. Lam, M.J. Ferguson, L. Deakin, A. Mar, Coord. Chem. Rev. 233–234 (2002) 207.
[2] A.M. Mills, A. Mar, Inorg. Chem. 39 (2000) 4599.
[3] O. Sologub, M. Vybornov, P. Rogl, K. Hiebl, G. Cordier, P. Woll, J. Solid State Chem. 122 (1996) 266.
[4] M.G. Morgan, M. Wang, A.M. Mills, A. Mar, J. Solid State Chem. 167 (2002) 41.
[5] G.M. Sheldrick, SHELXTL, Version 5.1, Bruker Analytical X-ray Systems, Inc. Madison, WI, 1997.
[6] International Tables for X-ray Crystallography, Vol. C, A.J.C. Wilson (Ed.), Kluwer, Dordrecht, 1992.
[7] M. O'Keeffe, N.E. Brese, Acta Crystallogr. B 48 (1992) 152.
[8] W. Jeitschko, R.O. Altmeyer, M. Schelk, U.Ch. Rotewald, Z. Anorg. Allg. Chem. 627 (2001) 1932.
[9] G. Papoian, R. Hoffmann, J. Solid State Chem. 139 (1998) 8.
[10] G.A. Papoian, R. Hoffmann, Angew. Chem. Int. Ed. 39 (2000) 2408.
[11] J. Donohue, The Structures of the Elements, Wiley, New York, 1974.
[12] W. Blase, G. Cordier, M. Somer, Z. Kristallogr. 199 (1992) 277.
[13] A.M. Mills, L. Deakin, A. Mar, Chem. Mater. 13 (2001) 1778.
[14] M. Somer, W. Carillo-Cabrera, J. Nuss, K. Peters, H.G. von Schnering, G. Cordier, Z. Kristallogr. 211 (1996) 479.
[15] R. Lam, R. McDonald, A. Mar, Inorg. Chem. 40 (2001) 952.
[16] R. Wang, H. Steinfink, Inorg. Chem. 6 (1967) 1685.
[17] G. Kimmel, D. Dayan, L. Zevin, J. Pelleg, Metall. Trans. A 16 (1985) 167.
[18] A.M. Mills, E.J. Anderson, A. Mar, J. Alloys Compd. 322 (2001) 103.
[19] T. Schmidt, W. Jeitschko, Inorg. Chem. 40 (2001) 6356.